

#### Contents lists available at ScienceDirect

# **HardwareX**





# FlumeX: A modular flume design for laboratory-based marine fluid-substrate studies

Melissa Ruszczyk <sup>a,b</sup>, Patrick M. Kiel <sup>c</sup>, Santhan Chandragiri <sup>a</sup>, Cedric M. Guigand <sup>d</sup>, Johnnie Xia Zheng <sup>a</sup>, Owen A. Brown <sup>a</sup>, Brian K. Haus <sup>d</sup>, Andrew C. Baker <sup>c</sup>, Margaret W. Miller <sup>e</sup>, Prannoy Suraneni <sup>f</sup>, Chris Langdon <sup>c</sup>, Vivek N. Prakash <sup>a,c,g,\*</sup> <sup>6</sup>

#### ARTICLE INFO

# Keywords: Laminar flows Flumes Flow tanks Corals Reefs Fluid-substrate Interface

#### ABSTRACT

As research becomes more interdisciplinary, researchers develop new methodologies and technologies for novel experiments that bridge fields. FlumeX's design features a standard experimental chamber that can be expanded into different configurations, allowing for cross-disciplinary experiments between the fields of fluid dynamics, chemical oceanography, and biology. An open-ended, flow-through configuration is ideal for simulating environments where water is constantly flushed, capable of simulating oceanic environments. A fully enclosed, recirculating configuration is ideal for particle image velocimetry experiments, standard for fluid dynamics. FlumeX is designed to allow for husbandry of sessile organisms, including corals, in tandem with chemical and physical measurements. FlumeX allows for flexibility in experimental design and comparable environments between recirculating and flow-through configurations. It is designed with low-cost, readily available materials, making it easy to build and produce en masse for replicate testing.

#### Specifications table

Hardware name	FlumeX	
Subject area	Chemistry, biochemistry	
-	Biological and ecological sciences	
	Environmental sciences	
	Fluid dynamics	
Hardware type	Flow characterization	

(continued on next page)

https://doi.org/10.1016/j.ohx.2025.e00697

Received 5 December 2024; Received in revised form 20 August 2025; Accepted 28 August 2025 Available online 29 August 2025

2468-0672/© 2025 The Authors. Published by Elsevier Ltd. This is an open access article under the CC BY-NC-ND license (http://creativecommons.org/licenses/by-nc-nd/4.0/).

<sup>&</sup>lt;sup>a</sup> Department of Physics, College of Arts & Sciences, University of Miami, Coral Gables, FL 33146, USA

<sup>&</sup>lt;sup>b</sup> Current Affiliation: Division of Natural Sciences and Mathematics, Keuka College, Keuka Park, NY 14478, USA

<sup>&</sup>lt;sup>c</sup> Department of Marine Biology and Ecology, Rosenstiel School of Marine, Atmospheric and Earth Science, University of Miami, Miami, FL 33149, USA

d Department of Ocean Sciences, Rosenstiel School of Marine, Atmospheric and Earth Science, University of Miami, Miami, FL 33149, USA

e SECORE International, Miami, FL 33145, USA

f Department of Civil and Architectural Engineering, College of Engineering, University of Miami, Coral Gables, FL 33146, USA

g Department of Biology, College of Arts & Sciences, University of Miami, Coral Gables, FL 33146, USA

<sup>\*</sup> Corresponding author at: Department of Physics, College of Arts & Sciences, University of Miami, Coral Gables, FL 33146, USA.. *E-mail address:* vprakash@miami.edu (V.N. Prakash).

(continued)

Hardware name	FlumeX
	Measuring physical properties
	Biological sample handling
Closest commercial analog	No commercial analog is available
Open-source license	Creative Commons Attribution-NonCommercial (CC BY-NC)
Cost of hardware	Experimental chamber: \$192.75 USD. Flow-through configuration* (2 flumes, digital flow meters): \$468.26 USD. Recirculating configuration*: \$355.37 USD. *Configuration estimates include cost of experimental chamber(s)
Source file repository	https://doi.org/10.5281/zenodo.14051748

#### 1. Hardware in context

Scientific research is increasingly becoming more interdisciplinary, necessitating integrative methods and materials to combine experimental practices from disparate fields. FlumeX is a modular flume designed to meet the experimental standards of fluid dynamics, chemical oceanography, and marine biology investigations – with each field bringing its own set of established protocols.

Fluid dynamics seeks to characterize hydrodynamic phenomena or environments. Researchers can quantify fluid flow in the lab by recording the movements of small, neutrally buoyant tracer particles and inferring flow characteristics using either Lagrangian methods of particle trajectory analysis (i.e., particle tracking velocimetry – PTV) [1], or using Eulerian methods of average particle behavior in a region (i.e., particle image velocimetry – PIV) [2]. These studies investigate flows in static tanks, wave tanks, or flumes, depending on the scale and nature of the investigated phenomenon. Each of these tools requires a transparent observational section for recording, and a constant volume of water to seed with tracer particles. Scientists then recreate specific hydrodynamic phenomena in these enclosed settings [3,4] and/or study flow around different physical structures [5–7]. Wave tanks are used to study larger scale wave mechanics [8,9]. Alternatively, flumes generate a unidirectional bulk flow and are advantageous to study benthic ecosystems [10,11]. Across these observational platforms, various tools including pumps and propellors drive pressure differences that develop reproducible, characteristic flows.

Chemical oceanography refers to the study of chemistry and chemical species within the ocean. Fundamental studies of the interactions between different chemical species and seawater can be carried out in controlled, lab-based experimental setups including flow reactors [12–15]. Field data can be analyzed on site using sensors and microelectrodes [16–18], or in the laboratory using standard lab equipment [19].

Studies in marine, and more generally aquatic, biology range from *in situ* observations in the field to controlled experiments in the laboratory. For many robust designs, biological experiments necessitate replicate sampling, multiple runs, and statistical hypothesis testing to quantify the data with sufficient statistical power due to inherent biological variation [20]. Replication is particularly salient in lab-based experiments, where additional known and unknown factors, such as animal handling and unmeasured environmental parameters, obfuscate changes in dependent variables [21,22].

As fluid dynamics, chemical oceanography, and marine biology intersect, new methods and sampling techniques are developed to accommodate the typical experimental designs of each field. Chemical reactions in flow can be studied in flow reactors which allow for studies of reactions with higher mixing rates and higher reactant concentrations than batch reactors [15]. There are a myriad of sensors and microelectrodes which collect chemical data in biological and fluid environments [18,23]. Fluorescent dyes or chemical tracers can be used in tandem with flow quantification to understand how chemical species are affected by hydrodynamic environments [24–26]. Biological organisms or their mimics are placed in tanks to record biogenic flow fields [27,28] or the effect of environmental flow on the organism [29–32]. For example, millimeter-scale topographic features were shown to affect coral larval settlement in wave-driven oscillatory flows [31]. Designing tools to jointly assess physical, chemical, and biological environs requires a tremendous, coordinated effort, often relying on separate quantifications and trials, plagued with untested assumptions of uniform hydrodynamics across multiple experimental apparatuses.

We have designed FlumeX – a modular flume system – which integrates the fields of fluid dynamics, chemistry, and biology, for simultaneous quantitative measurements. FlumeX features a standard observational, experimental chamber which can be fully assembled into different configurations, allowing for a consistent hydrodynamic environment between FlumeX configurations. FlumeX can be built in a flow-through configuration, optimal for chemical investigations under a consistent flow regime, or in a recirculating configuration, optimal for enclosed experiments including flow quantification. Biological experiments can occur in both configurations.

# 2. Hardware description

We present a flume design that can be modified for chemical, physical, and biological experiments occurring at small- to meso-scales (Reynolds number, Re, on a scale of  $10^2$ - $10^4$ ) of fluid motion close to the coral reef substrate interface. The focus is on the

near-substrate laminar boundary layer (cm scale), rather than the bulk region (m scale) where flows may be unsteady due to waves and turbulence. The flows in FlumeX intend to model near-substrate laminar boundary layer flows within a coral reef framework by matching flow speeds to those observed within a coral reef canopy  $(1-2 \text{ cm s}^{-1})$  [33–36].

Designing across disciplines poses its own unique set of limitations and design constraints, which need to be assessed in tandem with the broader experimental goals. FlumeX's design, including chemical sensors, flow measurements via PIV, and animal husbandry is shown in Fig. 1(a–c). The resulting design is based on the following features:

- A modular system, allowing for consistent measurements in an open (flow-through), or closed (recirculating) environment,
- An experimental chamber that produces steady, laminar flow across configurations,
- An inexpensive design that can easily be scaled up or down depending on experimental need (Fig. 1d-f).

The prominent and distinctive feature of FlumeX is its modular design. FlumeX is comprised of an experimental chamber that can be expanded with PVC pipe into two configurations – a closed, recirculating configuration, or an open, flow-through configuration. Laminar flow between configurations is consistent and repeatable, allowing for different types of measurements depending on the nature of the study. The closed, recirculating configuration is ideal for physical measurements including PIV. The open, flow-through configuration is ideal for chemical measurements in the lab that require a constant turnover or flushing of volume. Both the recirculating and flow-through configurations have an open and accessible experimental chamber allowing for easy care and husbandry of sessile organisms, including corals.

FlumeX is designed to mimic the hydrodynamic environment around newly settled corals, and therefore, is designed to operate at low to intermediate Re between  $10^2$  and  $10^4$  [37]. FlumeX produces steady, laminar flow across both configurations to successfully grow coral on various substrates while creating a hydrodynamic environment simulating ocean conditions for lab-based experiments.

FlumeX is made with low cost, easily accessible materials (primarily acrylic and PVC) available at local hardware stores, convenient for building replicate tanks with similar flow conditions. The presented design of FlumeX is built using 3 in, schedule-40 PVC pipes, but flume size can easily be scaled up or scaled down using different pipe dimensions depending on experimental need.

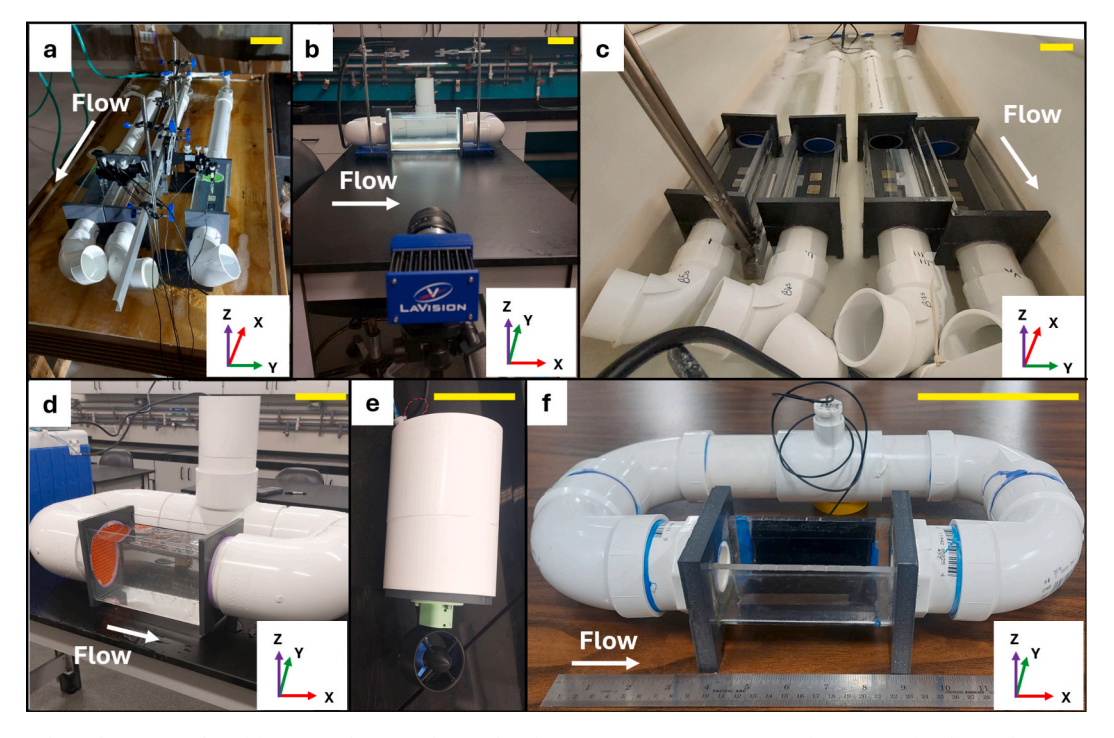


Fig. 1. Sample applications and modifications. FlumeX is designed with 3 in PVC pipe to (a) accommodate sensors for chemical measurements in a flow-through configuration, (b) collect physical, hydrodynamic measurements in a recirculating configuration, and (c) house biological organisms such as newly settled coral. FlumeX is easily (d, e) scaled up (pictured is FlumeX made with 6 in PVC pipe in a recirculating configuration), or (f) scaled down (pictured is FlumeX made with ½ in PVC pipe in a recirculating configuration), depending on experimental requirements. Yellow scale bar in each photo is 10 cm. (For interpretation of the references to colour in this figure legend, the reader is referred to the web version of this article.)

# 3. Design files summary

Design file name	File type	Open source license	Location of the file
viewingChamber.stl	3D Print File	CC BY-NC	https://doi.org/10.5281/zenodo.14051748
flowStraightener.stl	3D Print File	CC BY-NC	https://doi.org/10.5281/zenodo.14051748
mountingPlate.stl	3D Print File	CC BY-NC	https://doi.org/10.5281/zenodo.14051748
tileHolder.stl	3D Print File	CC BY-NC	https://doi.org/10.5281/zenodo.14051748
viewingChamber.dxf	CAD file	CC BY-NC	https://doi.org/10.5281/zenodo.14051748
tileHolder.dxf	CAD file	CC BY-NC	https://doi.org/10.5281/zenodo.14051748
mountingPlate.dxf	CAD file	CC BY-NC	https://doi.org/10.5281/zenodo.14051748

# 4. Bill of materials summary

# 4.1. Experimental chamber (EC): Builds one

Designator	Component	Number	Cost per unit – (USD)	Total cost – (USD)	Source of materials	Material type
EC1	12 in x 24 in x ¼ in acrylic sheet	1	\$21.69	\$21.69	https://www.mcmaster.com	Polymer
EC2	12 in x 24 in x 3/4 in PVC sheet; makes 2	1	\$74.49	\$74.49	https://www.mcmaster.com	Polymer
EC3	3 in PVC pipe	1	\$12.37	\$12.37	https://www.homedepot.com	Polymer
EC4	PLA plastic	1	\$20.99	\$20.99	https://www.amazon.com	Polymer
EC5	3/4 in x 4 in x 12 in PVC bar	1	\$23.82	\$23.82	https://www.mcmaster.com	Polymer
	Epoxy	1	\$7.48	\$7.48	https://www.homedepot.com	Other: Adhesive
	PVC primer/glue	1	\$10.94	\$10.94	https://www.homedepot.com	Other: Adhesive
	Silicone sealant	1	\$10.98	\$10.98	https://www.homedepot.com	Polymer
	Magnets (8 pack)	1	\$9.99	\$9.99	https://www.amazon.com	Metal

# 4.2. Flow-through configuration (FT): Two-line system

Some materials are listed twice, based on their location in the build – on the main line (FT-M) or on the flume line(s) (FT-F). Two options for flow meters are included – a digital and an analogue option – depending on need. PVC connections can be optionally reinforced with adhesive(s) listed in 4.1. Experimental chamber (EC) Bill of materials (PVC primer/glue, silicone sealant), depending on desired permanence.

Designato	r Component	Num	ber Cost per unit – (USD)	Total cost –(USD)	Source of materials	Material type
FT-M-1	Threaded hose to ¾ in PVC adaptor	1	\$1.05	\$1.05	https://www.homedepot.com	Polymer
FT-M-2	¾ in PVC pipe	1	\$3.16	\$3.16	https://www.homedepot.com	Polymer
FT-M-3	3/4 in PVC 90° elbow	1	\$0.79	\$0.79	https://www.homedepot.com	Polymer
FT-M-4	3/4 in PVC tee	1	\$0.82	\$0.82	https://www.homedepot.com	Polymer
FT-M-5	3/4 in PVC socket cap	1	\$0.82	\$0.82	https://www.homedepot.com	Polymer
FT-F-1	¾ in PVC pipe	1	\$3.16	\$3.16	https://www.homedepot.com	Polymer
FT-F-2	3/4 in PVC ball valve	2	\$3.22	\$6.44	https://www.homedepot.com	Polymer
FT-F-3	3/4 in PVC to threaded hose adap	tor 4	\$1.05	\$4.20	https://www.homedepot.com	Polymer
FT-F-4a	Flow meter (digital)	2	\$24.99	\$49.98	https://www.amazon.com	Other: Electrical
FT-F-4b	Flow meter (analog)	2	\$208.22	\$416.44	https://www.omega.com	Other: Mechanical
FT-F-5	3/4 in to 3 in PVC adaptor	2	\$5.86	\$11.72	https://www.mcmaster.com	Polymer
FT-F-6	3 in PVC pipe	2	\$12.37	\$24.74	https://www.homedepot.com	Polymer
FT-F-7	3 in PVC coupler	2	\$6.86	\$13.72	https://www.mcmaster.com	Polymer
EC	Experimental chamber	2	\$153.36	\$306.72	See Experimental chamber Bill of materials	Other: Mixed (see above)
FT-F-8	3 in PVC 90° elbow	2	\$9.50	\$19.00	https://www.mcmaster.com	Polymer
	PVC thread tape	1	\$1.96	\$1.96	https://www.homedepot.com	Other: Adhesive

#### 4.3. Recirculating configuration (R)

Attaching the propellor to the mounting plate can occur via extra adhesive(s) listed in 4.1. Experimental chamber (EC) Bill of materials or via screws as needed. PVC connections can be optionally reinforced with extra adhesive(s) listed in Experimental chamber (EC) Bill of materials (PVC primer/glue, silicone sealant), depending on desired permanence.

Designate	or Component	Numb	er Cost per unit – (USD	) Total cost –(USD)	Source of materials	Material type
R1	3 in PVC pipe	1	\$12.37	\$12.37	https://www.homedepot.com	Polymer
R2	3 in PVC coupler	2	\$6.86	\$13.72	https://www.mcmaster.com	Polymer
R3	3 in PVC 90° elbow	4	\$9.50	\$38.00	https://www.mcmaster.com	Polymer
R4	3 in PVC tee	1	\$13.93	\$13.93	https://www.mcmaster.com	Polymer
EC	Experimental chamber	1	\$153.36	\$153.36	See Experimental chamber Bill of materials	Other: Mixed (see above)
R5	6 in x 6 in x 3/4 in PVC sheet	1	\$12.65	\$12.65	https://www.mcmaster.com	Polymer
R6	3 in PVC pipe	1	\$12.37	\$12.37	https://www.homedepot.com	Polymer
R7	Propellor	1	\$22.99	\$22.99	https://www.amazon.com	Other: Electronic
R8	Power supply unit	1	\$65.99	\$65.99	https://www.amazon.com	Other: Electronic

#### 5. Build instructions

#### 5.1. Experimental chamber (EC, Fig. 2)

The experimental chamber (EC) and its components are consistent across the flow-through and recirculating configurations. The viewing chamber (EC1) serves as the observation chamber within the experimental chamber. To make the viewing chamber (EC1), cut a 30 cm  $\times$  40 cm rectangle from a  $\frac{1}{4}$  in acrylic sheet. Two scores along the width of the cut acrylic divide it into three rectangles – the outer rectangles measuring 30 cm  $\times$  14.5 cm, and the inner rectangle measuring 30 cm  $\times$  10 cm. Four circular wells are engraved in the corners of the middle rectangle on the same side as the scores to later help secure the tile-holder (EC5) during experiments. Evenly heat the acrylic along scores with a hot wire bender and bend to form 90° angles, creating a U-shape.

Cut two mounting plates (EC2) from a ¾ in PVC sheet. The mounting plates' design includes legs to create a stable base for the viewing chamber. Engrave a 1 cm wide U-shaped well into each mounting plate for the viewing chamber to rest in. Cut a horizontally centered circle matching the thickness of the tile-holder (EC5) – ¾ in – above the base of the U-shaped well to fit 3 in, schedule-40 PVC pipe within the channel. Attach the mounting plates to both ends of the viewing chamber by filling the U-shaped wells with quick-setting epoxy resin and fitting the viewing chamber into the wells. Cut two, 10 cm lengths of 3 in, schedule-40 PVC (EC3) to attach to each mounting plate. Attach each PVC pipe section to a mounting plate with PVA glue so they protrude outwards from the viewing chamber.

Use an FDM 3D printer to fabricate a 5 cm long flow straightener (EC4) with a diameter of 3 in to fit inside the one of the PVC pipe sections attached to the mounting plate. The flow straightener has a hexagonal grid (hexagon circumscribed diameter = 1 cm) ensuring laminar flow in the experimental chamber (Supplementary Fig. S1). Secure the flow straightener into one of the sections of 3 in PVC pipe using silicone, designating an upstream end of the experimental chamber and the resulting flow direction.

A tile-holder (EC5) nests substrate samples at the bottom of the viewing chamber creating a quasi-2-dimensional landscape, allowing for chemical and physical measurements on the surface of the substrate with no confounding effects resulting from 3-dimensional fluid interactions. The shape and type of substrates tested can alter the design of the tile-holder. The presented tile-holder design

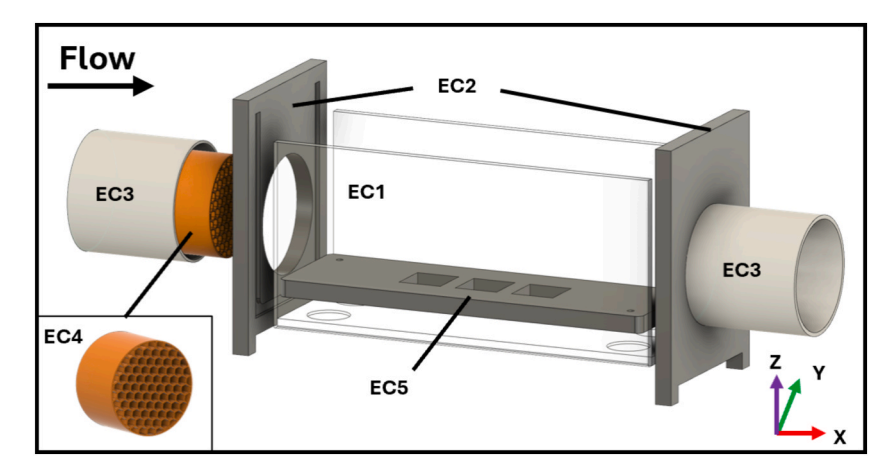


Fig. 2. Experimental chamber. Schematic of experimental chamber parts and assembly. The flow direction is determined based on the position of the flow straightener (EC4).

holds three,  $3 \text{ cm} \times 3 \text{ cm} \times 1 \text{ cm}$  tiles.

To make the tile-holder, cut a  $29 \text{ cm} \times 9.8 \text{ cm}$  section from a  $\frac{3}{4}$  in PVC sheet to fit the bottom of the tank, tangent to the bottom of the 3 in PVC inlet and outlet pipes. Engrave three  $3.2 \text{ cm} \times 3.2 \text{ cm} \times 1.3 \text{ cm}$  square recesses centered along the midline of the tile-holder and separated by 4.5 cm for sample substrate tiles. Centering the location for the tiles along the midline of the experimental chamber minimizes the hydrodynamic effects from the side walls of the viewing chamber (Supplementary Fig. S1c-e). In diagonal corners of the tile-holder, 1.5 cm from either edge, drill a threaded hole such that a  $\frac{1}{2}$  in threaded bolt can be used to help remove the tile-holder from the viewing chamber during experiments if needed.

Circular wells at the bottom of the viewing chamber are included as an optional feature to stabilize the tile-holder in strong flows. To utilize, attach 32 mm diameter, 3 mm tall circular magnets to the bottom of the tile-holder to align with the circular wells in the viewing chamber. Magnets will keep the tile-holder secured at the bottom of the tank. For extra stability, pair the magnets in the circular wells with magnets outside the viewing chamber to secure the tile-holder.

# 5.2. Flow-through configuration (FT, Fig. 3)

The flow-through (FT) configuration of FlumeX connects to a standard hose tap and features a main line (FT-M) which branches into multiple flume lines (FT-F). This design allows the flow-through configuration to support various installations depending on experimental need. The presented design describes the installation of a 2-line system, supporting two flumes.

#### 5.2.1. Main line (FT-M)

The main line connects to a hose via PVC adaptor (FT-M-1) and is made from alternating connecting  $\frac{3}{4}$  in, schedule-40 PVC pipes (FT-M-2) and socket tee joints (FT-M-3). Connecting  $\frac{3}{4}$  in PVC pipes are all 6 cm in length. The tee supports each branching flume line (FT-F). The final flume line connects to the main line via a 90° elbow (FT-M-4). If PIV is to be performed in the flow-through configuration, create a PIV inlet on FT-M between the outermost and penultimate flume lines by installing a tee joint vertically with an additional 10 cm length of PVC and a cap (FT-M-5). The PIV inlet allows for the addition of various materials to be added to the flow, including a high-density mixture of neutrally buoyant tracer particles for flow characterization via PIV in the outermost flume line.

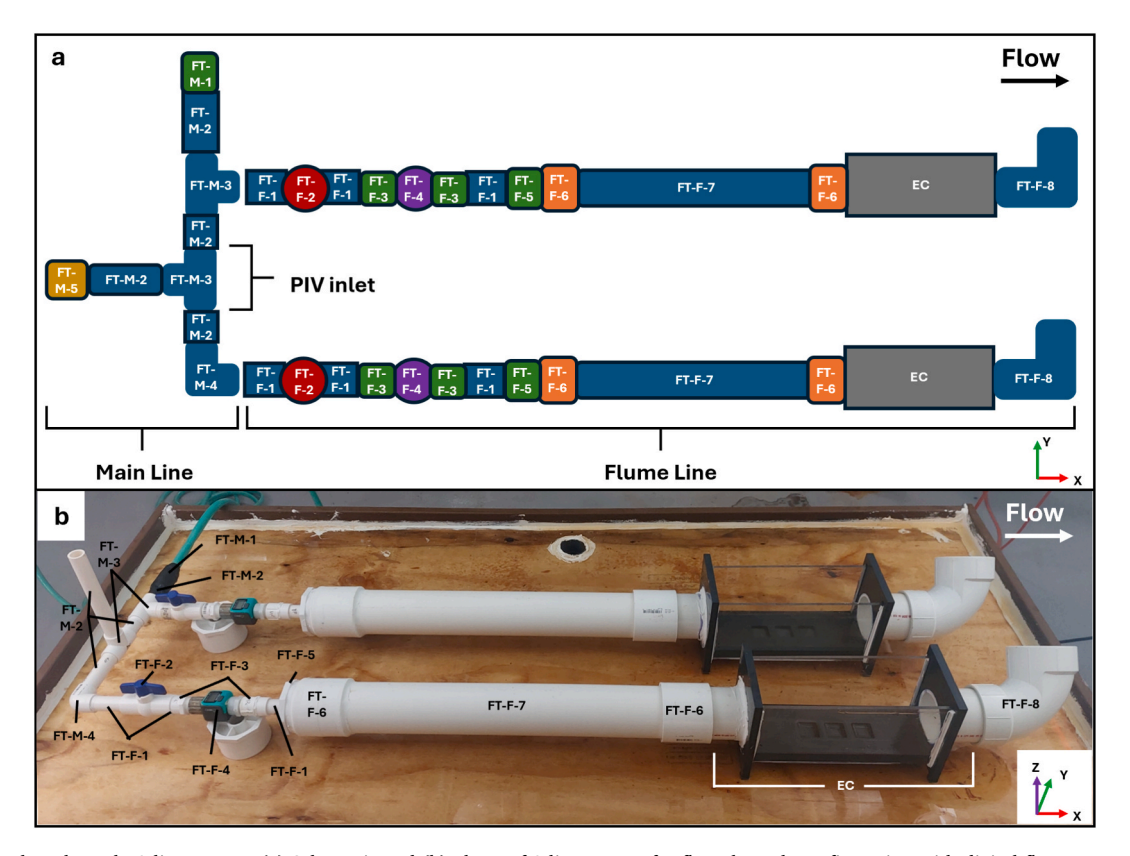


Fig. 3. Flow-through, 2-line system. (a) Schematic and (b) photo of 2-line system for flow-through configuration with digital flow meters. In the photo, only the bottom flume line is labeled for clarity, no PVC cap is pictured on the PIV inlet, and the hose connection (FT-M-1 and a section of FT-M-2) are wrapped in waterproof tape to prevent leaking.

#### 5.2.2. Flume line (FT-F)

Flume lines are constructed identically. Beginning from the main line, the flume line consists of ¾ in, schedule-40, connector PVC pipe (FT-F-1) connected to a ¾ in ball valve (FT-F-2). Following the ball valve is another length of ¾ in connector PVC pipe connected to a flow meter (FT-F-4) via a ¾ in PVC to threaded hose adaptor (FT-F-3). The flow meter connects back to ¾ in connector PVC pipe via another ¼ in PVC to threaded hose adaptor. The ¾ in PVC pipe then expands to support 3 in PVC pipe via a ¾ to 3 in PVC adaptor (FT-F-5). This adaptor connects to a 2 ft segment of 3 in, schedule-40 PVC pipe (FT-F-7) via a coupler (FT-F-6). At the opposite end of the 2 ft length of PVC pipe is another coupler that connects the pipe to the upstream end of the experimental chamber (EC). A 3 in PVC 90° elbow (FT-F-8) mounted on the downstream end of the experimental chamber controls outlet flow and consequently, the height of water in the viewing chamber.

The main line and flume lines upstream of the experimental chamber are made using  $\frac{3}{4}$  in PVC pipe which later expands to the 3 in PVC of the experimental chamber. This allows the flow-through configuration to be installed on common taps. Additionally, the  $\frac{3}{4}$  in pipe allows for easy measurements of the volumetric flow rate within the flumes, as instrumentation used to characterize flow in larger diameter pipes, including 3 in PVC pipes, are tuned to measure stronger flows than the target Re range of  $10^2-10^4$ . The ball valve on each flume line allows for precise control over the flow rate in individual flumes on the same line. Two different flow meter options are included in the Bill of Materials to measure flow rate – a cheaper digital flow meter for easy use (i.e., Fig. 3b), and a more expensive analog flow meter if the flumes are housed in a water bath (i.e., Fig. 1c).

#### 5.3. Recirculating configuration (R, Fig. 4)

The recirculating configuration is an enclosed design comprised of the experimental chamber (EC) and 3 in, schedule-40 PVC pipe (R1). Attach a 3 in, 90° elbow joint (R2) to the inlet of the experimental chamber, and another elbow joint (R2) to the outlet of the experimental chamber. The short sides of the recirculating configuration are made of 10 cm lengths of 3 in, schedule-40 PVC pipe (R1) connected to these elbows, with additional elbows at the end, forming a rectangular track. The far side of the track includes a 3 in PVC tee joint (R3) which connects halfway between the two elbows via 3 in PVC pipe (R1). The tee joint is installed such that the open end of the tee faces upwards to hold the propellor mount.

The propellor mount is a length of 3 in, schedule-40 PVC pipe (R5) with a plate to attach the propellor (R4) secured to the base of R5 via PVC glue. The plate has screw holes drilled into it to attach the propellor, and holes to run the electrical cabling of the propellor. Propellor cabling runs up through R4 and R5 and connects to an external power supply unit to control the voltage and amperage supplied to the propellor.

The recirculating configuration currently features no systematic way to set a target flow without PIV verification of the flow. Unlike the flow-through configuration which has sections of ¾ in PVC that can accommodate flow meters which measure low volumetric flow rates, the 3 in design of the recirculating configuration does not easily lend itself to a volumetric flow meter that can measure such low flow rates. However, modifications to FlumeX for experiments at different scales (i.e., smaller flume or faster flows) may allow for the installation and use of an inline flow meter for different hydrodynamic environments in the recirculating configuration.

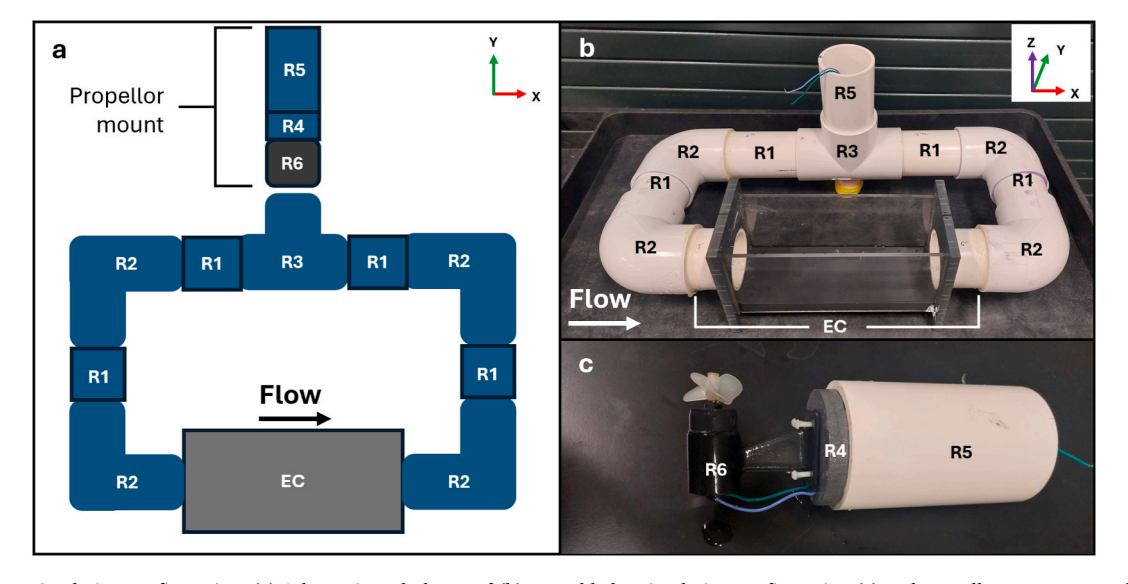


Fig. 4. Recirculating configuration. (a) Schematic and photos of (b) assembled recirculating configuration (c) and propellor mount. Note that the power supply unit is not included in the diagrams.

#### 6. Operation instructions

#### 6.1. Flow-through configuration

Ensure flume lines are level with the ground. Connect the flow-through main line to the water supply. Turn on the water supply and adjust pressure as needed via the main water supply and fine-tune the flow for each experimental chamber using the ball valves along each flume line. The volumetric flow rate can be observed via the flow meters installed along each flume line.

Due to the outflow design of the flumes, it is recommended they are used on a wet table or in a bath to contain the outflow of water. The wet table or bath can be connected to a drainage system for long-term use.

#### 6.2. Recirculating configuration

Ensure the experimental chamber is level with the ground. Fill the recirculating configuration with water. Control the flow of water via the power supplied to the propellor.

#### 7. Validation and characterization

#### 7.1. Computer simulations of laminar flows

During the initial design stage, COMSOL-based computer simulations were iteratively used to predict the flow conditions achievable in FlumeX, informing fabrication decisions. A CAD model of FlumeX's experimental chamber was imported into COMSOL. Flows within reefs can range from 1 cm s<sup>-1</sup> to 4 cm s<sup>-1</sup> [33,36,38]. The simulations here used an inlet velocity of 1 cm s<sup>-1</sup>, targeting the lower end of this range. Due to the lower target Re  $(10^2-10^4)$ , simulations were run with and without flow straighteners to determine if a flow straightener was worth incorporating into the final design. Simulations without a flow straightener were characterized by nonhomogeneous fluid flows in the viewing chamber, especially near the bottom side walls (Supplementary Fig. S1, c–e, left panels). Simulations that included a flow straightener upstream of the viewing chamber resulted in comparatively more homogeneous and laminar flows (Supplementary Fig. S1, c–e, right panels), particularly along the centerline (Supplementary Fig. S1e). Even with a flow straightener, flow profiles close to the side walls suffer unavoidable heterogeneities due to frictional effects from the walls (Supplementary Fig. S1, c–d). Hence, all fluid flow measurements and experiments are carried out along the center line of the viewing chamber (Supplementary Fig. S1e, right panel).

#### 7.2. 2-Dimensional particle image velocimetry (PIV)

Fluid flows and FlumeX configurations were verified and matched using 2-dimensional PIV. The experimental setup for carrying out PIV measurements is shown in Supplementary Fig. S2. Viewing chambers were illuminated with a 1350 lm LED illumination unit (LaVision) mounted above the experimental chamber creating a light sheet. The thickness of the light sheet was reduced to a 1 cm plane by adding an aperture to manually block incident light. An Imager CS2 5 camera mounted with a L 60 mm focal length lens (F/ 2.8, 2.1 macro, LaVision) with a full view of  $2448 \times 2064$  pixels recorded data. Flume verification took place over a cross section parallel to flow along the center line of the viewing chamber, spanning the width and height of the viewing chamber, resulting in a resolution across configurations of approximately  $80 \text{ px cm}^{-1}$ . Recordings in the flow-through configuration occurred at 40 Hz for 10 s and in the recirculating configuration at 20 Hz for 10 s.

Flumes were seeded with  $60 \mu m$  diameter polyamide tracer particles (LaVision). In the recirculating configuration, the entire volume of water in the flume was seeded in bulk, ensuring a constant seed density. In the flow-through configuration, a high-density mixture of polyamide particles was pipetted into the flume section at the PIV inlet and mixed with the water as it travelled through the flume line upstream of the experimental chamber. Recording was manually started once particles in the viewing chamber were at a near-uniform density. Multiple recordings were taken as the particles moved through the viewing chamber, and the recording with the most uniformly distributed particles was selected for PIV analysis.

Data was processed in DaVis 11.0.0.196 (LaVision). The PIV data post-processing in flow-through and recirculating configurations was performed using a bicubic interpolation to interpolate vectors,  $5 \times 5$  denoising, and a symmetrical shift correction mode. Pixels were interpolated using a spline interpolation and a direct correlation algorithm between frames, and cell sizes were weighted as a round cell. In the flow-through configuration, the window interrogation size was 64 px, resulting in an average correlation value of 0.84 px. In the recirculating configuration, the window interrogation size was 16 px, resulting in an average correlation value of 0.97 px.

#### 7.3. Matching flow conditions with theoretical fluid dynamics

Ten different flow conditions were tested in the flow-through configurations by varying the volumetric flow rate, and nine different flow conditions were tested in the recirculating configuration based on the voltage of the external power supply unit powering the propeller. Flow-through conditions ranged from 0.5 gal  $\min^{-1}$  (0.9 L  $\min^{-1}$ ) to 1.4 gal  $\min^{-1}$  (5.3 L  $\min^{-1}$ ) at 0.1 gal  $\min^{-1}$  (0.4 L  $\min^{-1}$ ) intervals based on the tolerance of the flow meter (based on U.S. units), and recirculating conditions ranged from the minimal voltage applied to power the propellor (0.90 V) to the voltage where the laminar flow began to break down and vortices in the

boundary layer appeared (1.30 V) at 0.05 V intervals. It is important to note that voltage measurements reported here will not be consistent over different installations of the recirculation configurations, as voltage and amperage depend on the number and type of electronics drawing from the same power source. Flow conditions within and across flume configurations were compared and matched by assessing boundary layer height, Reynolds number, maximum velocity, and average flow speed in the viewing chamber (Table 1).

Laminar boundary layers for the flows generated in FlumeX configurations were compared to the boundary layers predicted by theory to ensure the flows generated were laminar and matched theory as closely as possible. The boundary layer height, by definition, is the height normal to the substrate where flow velocity has reached 99 % of its freestream velocity [37]. The theoretical boundary layer height ( $\delta_{99}$ ) at location, X, downstream from the starting point of the experimental chamber (where X = 0), is calculated as:

$$\delta_{99}(X) pprox rac{5X}{\sqrt{Re_X}}; Re_X = rac{XV
ho}{\mu}$$
 (1)

where  $Re_X$  is the Reynolds number at location X, V is the maximum velocity in the entire tank for a given flow condition (m s<sup>-1</sup>),  $\rho$  is the fluid density (1024.26 kg m<sup>-3</sup>), and  $\mu$  is the dynamic viscosity of the fluid (1.027 × 10<sup>-3</sup>Pa s) [39]. To calculate the boundary layer height from experimental data, at each X-position along the length of the tank, the lowest height where the fluid reached 99 % of the freestream velocity along that profile was found. Boundary layer error was calculated for each flow condition at location, X, as the difference between the theoretical boundary layer height at X and the experimental boundary layer height at X (Fig. 5). The theoretical boundary layer heights across the viewing chamber range from 10.45 mm (minimum) to 17.69 mm (maximum) in height in the flow-through configuration, and from 14.54 mm (minimum) to 23.38 mm (maximum) in the recirculating configuration. FlumeX best matches the boundary layer in the upstream portions of the viewing chamber, and less towards the downstream end of the viewing chamber.

The average boundary layer error in the flow-through configuration is  $15.48 \pm 7.58$  mm and in the recirculating configuration is  $-2.64 \pm 6.09$  mm (mean  $\pm$  standard deviation). While the error observed in the recirculating configuration is close to zero, indicating that the hydrodynamic environment in FlumeX matches laminar theory well, the error in the flow-through configuration is higher. This may be a result of fluctuations in the flow coming into the system controlled by plumbing outside the build of FlumeX. Additionally, it is likely that uneven particle distribution using PIV techniques further skews the velocity fields. Although the PIV inlet is positioned early enough in the flow such that the particles are well-mixed, it is difficult to achieve a uniform particle field in the EC, as particles are still subject to velocity gradients within the flume line before the EC. Effective PIV is heavily dependent on uniform particle distribution, and regionally, areas with a lower density of particles including the fluid boundary layer, may be inaccurate and tend to have lower measured values than actual [40,41]. Lower velocity measurements in the boundary layer would result in the calculated boundary layer being higher than theory predicts. Although PIV in the flow-through configuration was performed on a reasonably even distribution of particles, the authors note that it was not a uniform distribution, comparable to measurements in the recirculating configuration. Although the average boundary layer height in the flow-through configuration is greater than in the recirculating configuration, this error falls within a reasonable limit, indicating that the hydrodynamic environments created in FlumeX – particularly in the recirculating configuration – match laminar theory quite well.

The Reynolds number was calculated for each tested flow condition as

$$Re = \frac{LV\rho}{\mu} \tag{2}$$

Table 1 Validation conditions. All tested hydrodynamic conditions for the flow-through and recirculating configurations of FlumeX. Where appropriate, data is presented as mean  $\pm$  standard deviation.

FlumeX configuration	External control parameter	Average boundary layer error (cm)	Experimental chamber Re	Maximum velocity (cm $s^{-1}$ )	Average flow speed (cm $s^{-1}$ )
Flow-through	0.5 gal min <sup>-1</sup>	$1.83\pm1.02$	660	2.20	$0.80 \pm 0.68$
_	$0.6 \text{ gal min}^{-1}$	$1.67\pm0.78$	820	2.75	$0.95 \pm 0.69$
	$0.7 \text{ gal min}^{-1}$	$1.71\pm0.64$	860	2.87	$1.11\pm0.82$
	$0.8~{ m gal~min^{-1}}$	$1.48\pm0.66$	880	2.94	$1.23\pm0.76$
	$0.9~{ m gal~min}^{-1}$	$1.61\pm0.67$	890	2.99	$1.28\pm0.89$
	$1.0~{ m gal~min}^{-1}$	$1.83\pm0.90$	990	3.31	$1.45\pm0.96$
	$1.1~{\rm gal~min}^{-1}$	$0.97\pm0.62$	1,200	3.95	$1.67\pm0.95$
	$1.2 \text{ gal min}^{-1}$	$1.50\pm0.70$	1,300	4.24	$1.96\pm1.01$
	$1.3~{\rm gal~min}^{-1}$	$1.43\pm0.54$	1,300	4.30	$1.96\pm1.10$
	$1.4~{ m gal~min^{-1}}$	$1.46\pm0.54$	1,400	4.55	$2.28\pm1.14$
Recirculating	0.90 V	$-0.26\pm0.25$	300	1.00	$0.55\pm0.25$
	0.95 V	$0.34\pm0.47$	380	1.27	$0.69 \pm 0.33$
	1.00 V	$-0.75 \pm 0.43$	470	1.58	$0.92\pm0.37$
	1.05 V	$-0.63 \pm 0.43$	550	1.83	$1.13\pm0.39$
	1.10 V	$0.01\pm0.81$	570	1.90	$1.09\pm0.49$
	1.15 V	$-0.26 \pm 0.54$	660	2.19	$1.31 \pm 0.50$
	1.20 V	$-0.52 \pm 0.38$	700	2.36	$1.41\pm0.53$
	1.25 V	$-0.12\pm0.44$	790	2.65	$1.55\pm0.61$
	1.30 V	$-0.19\pm0.70$	760	2.54	$1.42\pm0.57$

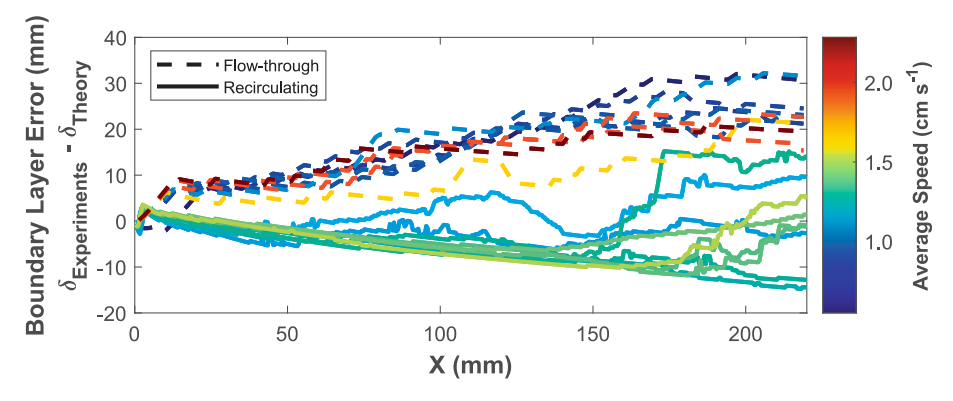


Fig. 5. Boundary layer error. Boundary layer error ( $\delta_{Experiments} - \delta_{Theory}$ ) at flume length, X, tested at different conditions in the flow-through (dashed lines) and recirculating (solid lines) configurations. The different cases are colored coded by their average bulk flow speed.

with L as the length of the viewing chamber (0.30 m). Reynolds number in the flow-through configuration ranged from 660 to 1400 and from 300 to 760 in the recirculating configuration. These numbers fall within the target range of Reynolds numbers between  $10^2$  and  $10^4$  for laminar flow conditions on coral reefs [37,38].

Flow velocity data was used to match hydrodynamic landscapes between flume configurations. Velocity profiles were averaged over time to generate the average velocity profiles for different conditions in the flow-through and recirculating configurations (Fig. 6, Supplementary Figs. S3 and S4). Average flow speed was calculated by averaging all speed measurements across time and location in the viewing chamber. Maximum velocities in the flow-through configuration ranged from  $2.20 \, \mathrm{cm \ s^{-1}}$  to  $4.55 \, \mathrm{cm \ s^{-1}}$  and from  $1.00 \, \mathrm{cm \ s^{-1}}$ 

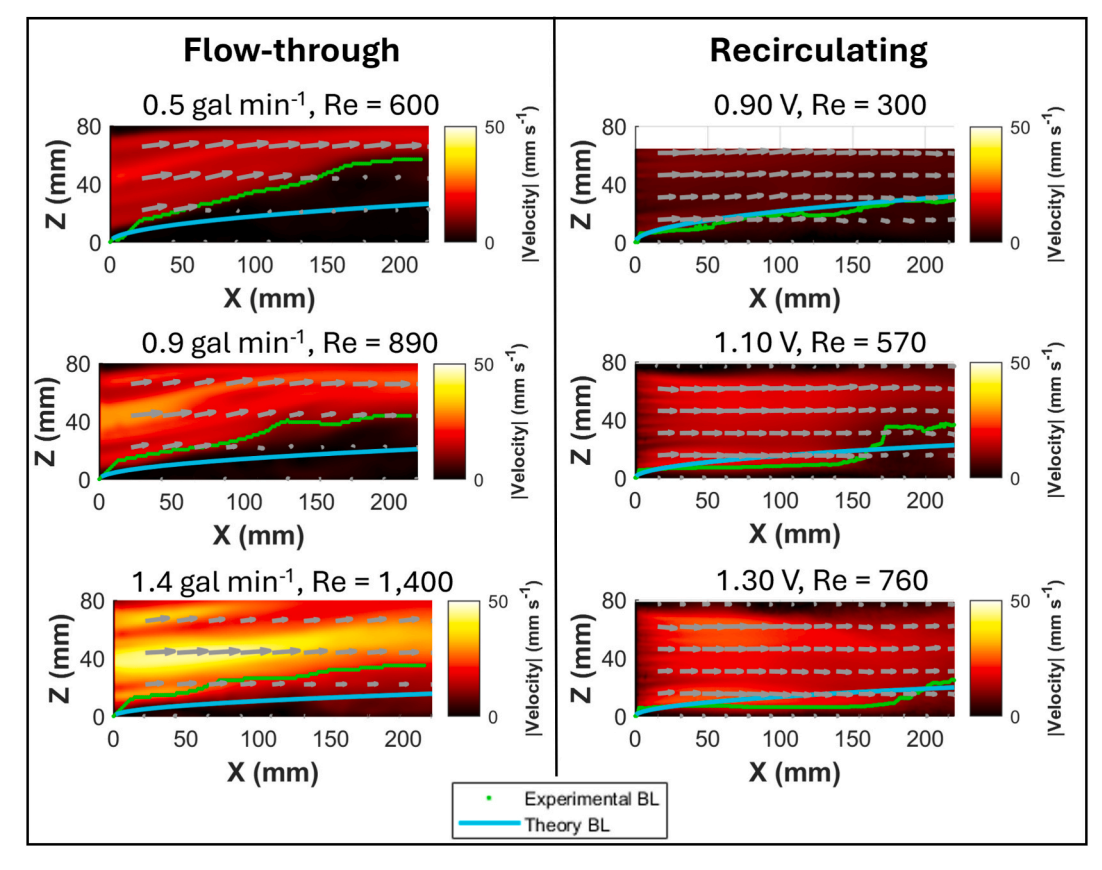


Fig. 6. Flume Verification. Velocity profiles for the lowest (top), middle (middle), and highest (bottom) flow conditions tested in the flow-through (left) and recirculating (right) configurations of FlumeX with velocity vectors overlayed. The boundary layers (BL) calculated in the experiment based on observed flow conditions (green) and calculated from theory (blue) are overlayed on the figures. A greater upper limit was tested in the flow-through configuration than the recirculating configuration, and a lesser lower limit was tested in the recirculating configuration than the flow-through configuration. (For interpretation of the references to colour in this figure legend, the reader is referred to the web version of this article.)

cm s $^{-1}$  to 2.54 cm s $^{-1}$  in the recirculating configuration. Average flow speed ranged from 0.80 cm s $^{-1}$  to 2.28 cm s $^{-1}$  in the flow-through configuration and from 0.55 cm s $^{-1}$  to 1.42 cm s $^{-1}$  in the recirculating configuration. By adjusting and cross-referencing these data between FlumeX's configurations, it is possible to obtain similar flows across flume configurations.

#### CRediT authorship contribution statement

Melissa Ruszczyk: Writing – review & editing, Writing – original draft, Visualization, Validation, Methodology, Investigation, Formal analysis, Data curation, Conceptualization. Patrick M. Kiel: Writing – review & editing, Visualization, Software, Methodology, Investigation, Conceptualization. Santhan Chandragiri: Visualization, Software, Methodology, Investigation, Conceptualization. Cedric M. Guigand: Visualization, Software, Resources, Methodology, Conceptualization. Johnnie Xia Zheng: Methodology, Investigation. Owen A. Brown: Methodology, Investigation. Brian K. Haus: Resources, Project administration. Andrew C. Baker: Supervision, Project administration, Funding acquisition. Margaret W. Miller: Writing – review & editing, Supervision, Project administration. Chris Langdon: Supervision, Resources, Project administration. Vivek N. Prakash: Writing – review & editing, Supervision, Software, Resources, Project administration, Funding acquisition, Conceptualization.

# Declaration of competing interest

The authors declare that they have no known competing financial interests or personal relationships that could have appeared to influence the work reported in this paper.

# Acknowledgments

The authors would like to acknowledge all members of the XREEFs team for their support, in particular Dr. Sanchit Mehta and the students in the SUSTAIN laboratory at the University of Miami, as well as members of the Prakash Lab for useful discussions. The authors also thank Dr. Douglas Neal from LaVision Inc, for installation and support of the PIV system. P.S. and V.N.P. acknowledge funding support from the University of Miami Laboratory for Integrative Knowledge (U-LINK) project "Improving Coral Larval Recruitment using Engineering, Biophysics, and Generative AI". V.N.P. would also like to acknowledge start-up funding support from the University of Miami.

This material is based upon work supported by the Defense Advanced Research Projects Agency under the Reefense Program, BAA HR001121S0012. The views, opinions and/or findings expressed are those of the author and should not be interpreted as representing the official views or policies of the Department of Defense or the U.S. Government.

# Declaration of generative AI and AI-assisted technologies

No AI or generative AI was used in preparation of the manuscript. The authors wrote, reviewed, and edited the content, and take full responsibility for the content of the published article.

#### Appendix A. Supplementary data

Supplementary data to this article can be found online at https://doi.org/10.1016/j.ohx.2025.e00697.

# References

- [1] N.T. Ouellette, H.T. Xu, E. Bodenschatz, A quantitative study of three-dimensional Lagrangian particle tracking algorithms, Exp. Fluids 40 (2) (Feb 2006) 301–313, https://doi.org/10.1007/s00348-005-0068-7.
- [2] R. J. Adrian and J. Westerweel, Particle Image Velocimetry (Cambridge Aerospace Series, no. 30). Cambridge, U.K.: Cambridge University Press, 2011, p. 586.
- [3] M.S. Islam, K. Haga, M. Kaminaga, R. Hino, M. Monde, Experimental analysis of turbulent flow structure in a fully developed rib-roughened rectangular channel with PIV, Exp. Fluids 33 (2) (Aug 2002) 296–306, https://doi.org/10.1007/s00348-002-0432-9.
- [4] C.M. Velte, C. Braud, S. Coudert, J.M. Foucaut, Vortex generator induced flow in a high Re boundary layer, J. Phys. Conf. Ser. 555 (2014), https://doi.org/10.1088/1742-6596/555/1/012102.
- [5] G.E. Elsinga, J. Westerweel, Tomographic-PIV measurement of the flow around a zigzag boundary layer trip, Exp. Fluids 52 (4) (Apr 2012) 865–876, https://doi.org/10.1007/s00348-011-1153-8.

[6] G. Misuriya, T.I. Eldho, B.S. Mazumder, Experimental investigations of turbulent flow characteristics around different cylindrical objects using PIV measurements, Eur. J. Mech. B-Fluid 101 (2023) 30–41, https://doi.org/10.1016/j.euromechflu.2023.05.001.

- [7] M. Lewis, E. Silver, R. Hunt, D.M. Harris, OpenFlume: An accessible and reproducible benchtop flume for research and education, HardwareX 20 (2025) e00583.
- [8] A. Robinson, D. Ingram, I. Bryden, T. Bruce, The generation of 3D flows in a combined current and wave tank, Ocean Eng. 93 (2015) 1–10, https://doi.org/10.1016/j.oceaneng.2014.10.008.
- [9] Y.T. Wu, S.C. Hsiao, Generation of stable and accurate solitary waves in a viscous numerical wave tank, Ocean Eng. 167 (2018) 102–113, https://doi.org/ 10.1016/j.oceaneng.2018.08.043.
- [10] S. Comeau, et al., Flow-driven micro-scale pH variability affects the physiology of corals and coralline algae under ocean acidification, Sci. Rep.-Uk 9 (2019), https://doi.org/10.1038/s41598-019-49044-w.
- [11] J.L. Falter, et al., A novel flume for simulating the effects of wave- and tide-driven water motion on the biogeochemistry of benthic reef communities, Limnol. Oceanogr.-Meth. 4 (Apr 2006) 68–79, https://doi.org/10.4319/lom.2006.4.68.
- [12] C. Langdon, R. Albright, A.C. Baker, P. Jones, Two threatened Caribbean coral species have contrasting responses to combined temperature and acidification stress, Limnol. Oceanogr. 63 (6) (Nov 2018) 2450–2464, https://doi.org/10.1002/ino.10952.
- [13] J.E. Campbell, J.D. Craft, N. Muehllehner, C. Langdon, V.J. Paul, Responses of calcifying algae (spp.) to ocean acidification: Implications for herbivores, Mar. Ecol. Prog. Ser. 514 (2014) 43–56, https://doi.org/10.3354/meps10981.
- [14] M.H. Kaufman, J.G. Wardeb, M.B. Cardenas, J.C. Stegen, E.M. Graham, J. Brown, Evaluating a laboratory flume microbiome as a window into natural riverbed biogeochemistry, Front. Water 3 (2021) 596260.
- [15] P. Watts, C. Wiles, Micro reactors, flow reactors and continuous flow synthesis, J. Chem. Res. 181 (2012) 181-193.
- [16] C.E. Reimers, Applications of microelectrodes to problems in chemical oceanography, Chem. Rev. 107 (2) (Feb 2007) 590–600, https://doi.org/10.1021/cr050363n.
- [17] T. Fukuba, T. Fujii, Lab-on-a-chip technology for combined observations in oceanography, Lab Chip 21 (1) (2021) 55-74, https://doi.org/10.1039/d0lc00871k.
- [18] Y.Q. Liu, H.L. Lu, Y. Cui, A review of marine in situ sensors and biosensors, J Mar. Sci. Eng. 11 (7) (2023), https://doi.org/10.3390/jmse11071469.
- [19] P. Fourrier, et al., Characterization of the vertical size distribution, composition and chemical properties of dissolved organic matter in the (ultra)oligotrophic Pacific Ocean through a multi-detection approach, Mar. Chem. 240 (2022), https://doi.org/10.1016/j.marchem.2021.104068.
- [20] P.G. Beninger, I. Boldina, S. Katsanevakis, Strengthening statistical usage in marine ecology, J. Exp. Mar. Biol. Ecol. 426 (2012) 97–108, https://doi.org/10.1016/j.jembe.2012.05.020.
- [21] K.A. Sloman, J.D. Armstrong, Physiological effects of dominance hierarchies: laboratory artefacts or natural phenomena? J. Fish Biol. 61 (1) (Jul 2002) 1–23, https://doi.org/10.1006/jfbi.2002.2038.
- [22] H. Finn, M. Maxwell, M. Calver, Why does experimentation matter in teaching ecology? J. Biol. Educ. 36 (4) (2002) 158–162, https://doi.org/10.1080/00219266.2002.9655826.
- [23] R.L. Hartman, J.P. McMullen, K.F. Jensen, Deciding whether to go with the flow: Evaluating the merits of flow reactors for synthesis, Angew. Chem. Int. Ed. 50 (33) (2011) 7502–7519.
- [24] J.P. Crimaldi, Planar laser induced fluorescence in aqueous flows, Exp. Fluids 44 (6) (Jun 2008) 851-863, https://doi.org/10.1007/s00348-008-0496-2.
- [25] D.L. Young, A.I. Larsson, D.R. Webster, Structure and mixing of a meandering turbulent chemical plume: Concentration and velocity fields, Exp. Fluids 62 (12) (2021), https://doi.org/10.1007/s00348-021-03337-x.
- [26] N. Riviere, S. Pouchoulin, W. Cai, G.L. Kouyi, J. Le Coz, E. Mignot, A new pH-based tracing method for flow mixing studies in closed-loop experimental flumes: evaluation in an open-channel confluence, Environ. Fluid Mech. 14 (2024), https://doi.org/10.1007/s10652-024-09990-0.
- [27] P.M. Kiel, V.N. Prakash, Coral physiology: Going with the ciliary flow, Curr. Biol. 32 (19) (2022), https://doi.org/10.1016/j.cub.2022.08.049.
- [28] P. Xiong, J.H. Deng, X.Y. Chen, Performance improvement of hydrofoil with biological characteristics: Tail fin of a whale, Processes 9 (9) (2021), https://doi. org/10.3390/pr9091656.
- [29] H. Tu, F.J. Wang, H.P. Wang, Q. Gao, R.J. Wei, Experimental study on wake flows of a live fish with time-resolved tomographic PIV and pressure reconstruction, Exp. Fluids 63 (1) (2022), https://doi.org/10.1007/s00348-021-03378-2.
- [30] M. Ruszczyk, D.R. Webster, J. Yen, The response of a freshwater copepod to small-scale, dissipative eddies in turbulence, Limnol. Oceanogr. 13 (2023), https://doi.org/10.1002/lno.12402.
- [31] M.A. Levenstein, et al., Millimeter-scale topography facilitates coral larval settlement in wave-driven oscillatory flow, PLoS One 17 (9) (2022) e0274088, https://doi.org/10.1371/journal.pone.0274088.
- [32] M. Ruszczyk, et al., Local alkalinity enhancement using artificial substrates increases survivorship of early-stage coral recruits, bioRxiv (2025).
- [33] S. Chang, C. Elking, M. Alley, J. Eaton, S. Monismitha, Flow inside a coral colony measured using magnetic resonance velocimetry, Limnol. Oceanogr. 54 (2009) 1819–1827
- [34] C.O. Pacherres, S. Ahmerkamp, G.M. Schmidt-Grieb, M. Holtappels, C. Richter, Ciliary vortex flows and oxygen dynamics in the coral boundary layer, Sci. Rep.-Uk 10 (7541) (2020).
- [35] M.A. Reidenbach, J.R. Koseff, S.G. Monismith, Laboratory experiments of fine-scale mixing and mass transport within a coral canopy, Phys. Fluids 19 (2007) 075107.
- [36] I.C. Enochs et al., "Coral persistence despite marginal conditions in the Port of Miami," Sci Rep-Uk, vol. 13, no. 1, Apr 25 2023, doi: 10.1038/s41598-023-33467-7.
- [37] B.R. Munson, T.H. Okiishi, W.W. Huebsch, A.P. Rothmayer, Fundamentals of Fluid Mechanics, 7 ed., Wiley, 2013, p. 792.
- [38] N. Shashar, S. Kinane, P.L. Jokiel, M.R. Patterson, Hydromechanical boundary layers over a coral reef, J. Exp. Mar. Biol. Ecol. 199 (1) (Jul 1996) 17–28, https://doi.org/10.1016/0022-0981(95)00156-5.
- [39] H. Schlichting, Boundary Layer Theory, 7th ed., McGraw-Hill College, 1979.
- [40] C.J. Kähler, S. Scharnowski, C. Cierpka, On the uncertainty of digital PIV and PTV near walls, Experimental Fluids 52 (2012) 1641-1656.
- [41] R. Hain, C.J. Kähler, Fundamentals of multiframe particle image velocimetry (PIV), Exp. Fluids 42 (4) (Apr 2007) 575–587, https://doi.org/10.1007/s00348-007-0266-6.



Melissa Ruszczyk is currently a Visiting Assistant Professor of Biology in the Division of Natural Sciences and Mathematics at Keuka College, NY. FlumeX was designed during her work as a postdoctoral researcher working with Prof. Vivek N. Prakash in the Department of Physics at the University of Miami, FL. Her research focuses on how organisms' physical environments affect their resulting morphology and ecology, particularly in planktonic organisms. Dr. Ruszczyk received her B.S. in Biology and Music from Allegheny College, PA and her Ph.D. in Ocean Science and Engineering with a minor in Applied Mathematics from the Georgia Institute of Technology, GA.



Patrick M. Kiel is a Ph.D. candidate in Marine Biology and Ecology (MBE) at the University of Miami's Rosenstiel School for Marine, Atmospheric and Earth Science. His interdisciplinary research bridges marine biology, physics and engineering to uncover mechanisms underlying coral persistence and reveal insights that can directly inform restoration strategies and conservation initiatives. Patrick is co-advised by University of Miami faculty Prof. Vivek N. Prakash, Prof. Prannoy Suraneni, Prof. Diego Lirman, and Dr. Ian Enochs at NOAA.



Santhan Chandragiri is a postdoctoral researcher working with Prof. Vivek N. Prakash in the Department of Physics at the University of Miami, FL. Dr. Chandragiri obtained his Ph.D. in Chemical Engineering for his research on active fluid flows from the Indian Institute of Technology Madras, India. After his Ph.D., he started to work in the field of marine biophysics, specifically on experimental and theoretical biological fluid mechanics of ciliated marine larvae at the University of Miami. He is also interested in working on topics in soft matter such as the coffee ring effect.



Vivek N. Prakash is an Assistant Professor in the Department of Physics, and a secondary faculty in the Departments of Biology, and Marine Biology & Ecology (Rosenstiel School) at the University of Miami, FL. His research at the interface of Physics and Biology is driven by a sense of curiosity, fascination and discovery. Previously, he carried out Postdoctoral research in Biomechanics at Stanford University. He received his Ph.D. in Applied Physics from the University of Twente, The Netherlands. He obtained his master's and undergraduate degrees in Engineering Mechanics and Mechanical Engineering in India.